Journal of Anatomy

J. Anat. (2010) **216**, pp368–380 doi: 10.1111/j.1469-7580.2009.01177.x

Deep evolutionary roots of strepsirrhine primate labyrinthine morphology

Renaud Lebrun,[1,2,3] Marcia P. de León,[1] Paul Tafforeau[4] and Christoph Zollikofer[1]

[1]*Anthropologisches Institut und Museum, Universität Zürich-Irchel, Zürich, Switzerland*
[2]*Institut des Sciences de l'Evolution de Montpellier, Université Montpellier II, Montpellier, France*
[3]*Institut International Paléoprimatologie et Paléontologie Humaine, Evolution et Paléoenvironnements, UMR 6046 C.N.R.S. & Université de Poitiers, Poitiers, France*
[4]*European Synchrotron Radiation Facility, Grenoble, France*

Abstract

The cavity system of the inner ear of mammals is a complex three-dimensional structure that houses the organs of equilibrium and hearing. Morphological variation of the inner ear across mammals reflects differences in locomotor behaviour and hearing performance, and the good preservation of this structure in many fossil specimens permits analogous inferences. However, it is less well known to what extent the morphology of the bony labyrinth conveys information about the evolutionary history of primate taxa. We studied this question in strepsirrhine primates with the aim to assess the potential and limitations of using the inner ear as a phylogenetic marker. Geometric morphometric analysis showed that the labyrinthine morphology of extant strepsirrhines contains a mixed locomotor, allometric and phylogenetic signal. Discriminant analysis at the family level confirmed that labyrinthine shape is a good taxonomic marker. Our results support the hypothesis that evolutionary change in labyrinthine morphology is adequately described with a random walk model, i.e. random phenotypic dispersal in morphospace. Under this hypothesis, average shapes calculated for each node of the phylogenetic tree give an estimate of inner ear shapes of the respective last common ancestors (LCAs), and this information can be used to infer character state polarity. The labyrinthine morphology of the fossil Adapinae is close to the inferred basal morphology of the strepsirrhines. The inner ear of *Daubentonia*, one of the most derived extant strepsirrhines, is autapomorphic in many respects, but also presents unique similarities with adapine labyrinths.

Key words Adapiformes; geometric morphometrics; inner ear; primates; strepsirrhini.

Introduction

The inner ear of mammals follows a consistent bauplan but exhibits substantial morphological variation across taxa, which is typically seen as the result of adaptation to different functional contexts. Differences in cochlear coiling and in the relative size of the semicircular canals are correlated with differences in auditory capacities (Steele & Zais, 1985; West, 1985) and locomotor behaviour (Matano et al. 1985, 1986; Spoor et al. 1994; Spoor & Zonneveld, 1998), respectively. Specifically, a narrow apical relative to the basal turn of the cochlea is correlated with an extended low-frequency hearing limit (Manoussaki et al. 2008), and relatively large semicircular canals are correlated with fast, jerky styles of locomotion (Spoor et al. 2002, 2007). Because the labyrinth is contained in the densely ossified petrous bone it is often integrally preserved in fossil specimens, which allows inferences on locomotion (Spoor et al. 1994, 2007; Spoor & Zonneveld, 1998; Walker et al. 2008; Silcox et al. 2009) and also on hearing in extinct species (Rosowski & Graybeal, 1991; Ketten, 1992; Meng & Fox, 1995; Fox & Meng, 1997; Manoussaki et al. 2008). While the functional significance of the primate labyrinth has been investigated in great detail, still relatively little is known about its phylogenetic significance (Spoor, 1993; Hublin et al. 1996; Spoor et al. 2003). Labyrinthine morphology may exhibit marked differences between closely related taxa with similar patterns of locomotion, such as for example *Homo sapiens* and *Homo neanderthalensis* (Hublin et al. 1996; Spoor et al. 2003), indicating that the morphology of the inner ear – like that of the surrounding temporal bone (Lockwood et al. 2004) – contains a significant phylogenetic signal.

In cases where morphology-based analyses yield conflicting results due to homoplasy, molecular data provide independent evidence of phylogenetic relationships. In such

Correspondence
Renaud Lebrun, Anthropologisches Institut und Museum, Universität Zürich-Irchel, Winterthurerstrasse 190, 8057 Zürich, Switzerland.
E: lebrun@aim.uzh.ch

Accepted for publication *23 October 2009*
Article published online *21 December 2009*

cases, the analysis of neutral molecular markers can often resolve phyletic issues. In fossils, only morphology is available, and it is sensible to calibrate phene-based trees comprising fossil taxa with gene-based trees of actual taxa. Such an approach also permits *a posteriori* refinement of the choice of the morphological characters which are used for the purpose of phylogenetic reconstructions (Pilbeam, 1997). Studies analyzing the morphological variation in the light of the molecular evidence have already proven useful in identifying phenetic features characteristic for the human–chimpanzee clade (Gibbs et al. 2002; Lockwood et al. 2004; Bradley, 2008), and in the search for cranial features reflecting hominin phylogeny (González-Jose et al. 2008) and modern human phylogeography (Harvati & Weaver, 2006; Manica et al. 2007; Roseman & Weaver, 2007; Smith et al. 2007; Betti et al. 2009; Romero et al. 2009). Furthermore, geometric morphometric methods offer new possibilities to study the phylogenetic signal contained in morphology because these methods permit comprehensive quantification of morphological features, which are traditionally described as an array of characters with discrete states. We adopt such an approach in the present study.

The molecular phylogeny of extant strepsirrhines is well documented (Yoder et al. 1996, 2000; Yoder, 1997; Pastorini et al. 2001, 2002, 2003; Poux & Douzery, 2004; Roos et al. 2004; Yoder & Yang, 2004). Furthermore, adaptive radiation within each major strepsirrhine group led to a wide spectrum of locomotor specializations (Martin, 1972; Rasmussen & Nekaris, 1998) such that extant strepsirrhine diversity represents an ideal testbed to assess functional vs. phylogenetic factors influencing the morphology of the bony labyrinth. Within fossil primates, the Adapiformes most likely represent the sister group of the strepsirrhines (Kay et al. 1997; Yoder, 1997; Godinot, 1998; Rasmussen & Nekaris, 1998; Marivaux et al. 2001; Seiffert et al. 2003, 2009; Seiffert, 2005), and the morphology of their inner ear may thus be a good model of the ancestral morphology of the strepsirrhine inner ear. Also, the Adapinae bear evidence of a wide range of locomotor behaviours (Bacon & Godinot, 1998; but see also Dagosto, 1983, 1993 and Gebo, 1983) such that investigation of their labyrinthine morphology can provide additional evidence on how function affects variation in this structure. In addition, the recent description of a well preserved Eocene primate, *Darwinius masillae*, has revived the debate on the phylogenetic relationships of Adapiformes and extant primates (Franzen et al. 2009). Investigation of the morphological affinities between the labyrinthine morphology of Adapiformes and extant primates may thus also help to clarify the phylogenetic position of this extinct primate group.

Here, we first assess the strength of the phyletic signal contained in the inner ear and in other potentially functionally constrained cranial structures of extant primate taxa, and in particular of strepsirrhines, using neutral molecular markers as a reference. Based on this evidence, we then assess the potential and limitations of using the morphology of the inner ear as a taxonomic marker, and as a phylogenetic marker to reconstruct evolutionary relationships among extant and extinct strepsirrhine families.

Materials and methods

Sample composition

The sample consisted of 38 strepsirrhine cranial specimens, which represent all extant lemuriform and lorisiform genera, and of nine fossil specimens, representing three genera belonging to the Adapinae subfamily [*Adapis* (n = 7), *Palaeolemur* (n = 1), and *Leptadapis* (n = 1)] (see Table 1). Inner ears of 10 haplorhine specimens [Tarsiidae (n = 4), Cebidae (n = 2), Cercopithecidae (n = 2), Hominidae (n = 2)] were also included for comparison. Additionally, four specimens belonging to the orders Scandentia and Dermoptera, the sister groups of the primate order (Waddell et al. 1999; Madsen et al. 2001; Janecka et al. 2007), were included. Left and right inner ears were integrated in the sample when preserved. All but three specimens are adults (the three being subadults). As a whole, three-dimensional labyrinthine and cranial morphologies were quantified in a sample of 61 specimens.

Data acquisition

Digital volume data of all specimens were acquired using X-ray micro-computed tomography (μCT), synchrotron X-ray microtomography (SR-μCT) and conventional computed tomography (CT). Most fossil specimens were scanned at the European Synchrotron Radiation Facility (ESRF) on beam lines ID17 and ID19 (see Table 1). Using synchrotron tomography for highly mineralized fossils resulted in high contrast and spatial resolutions, which greatly facilitated segmentation of the bony labyrinth cavities filled by dense sediment (Tafforeau et al. 2006). Extant specimens were scanned with a Scanco μCT80 microtomographic device, with a microtomographic device at the Swiss Federal Laboratories for Materials Testing and Research (EMPA), and with a medical scanner (see Table 1). Following volume data segmentation with AMIRA 3.1.1 (Mercury Systems, Inc.) via thresholding and manual segmentation, 3D surfaces representing the entire cranium and the bony labyrinths were reconstructed.

The labyrinthine form was quantified with 22 anatomical landmarks distributed approximately equally over the entire bony labyrinth (Fig. 1, Table 2). Choosing a single threshold value could affect to some extent the reconstruction of the semicircular canals and of the cochlea, because the CT numbers in the air-filled semicircular canals often do not reach the true value of air (Spoor & Zonneveld, 1995), whereas in other parts of the labyrinths such as the cochlea the value of air is reached. To minimize that effect, landmarks were located at the centres of the lumina of the semicircular canals, of the ampullae, and of the cochlear helix. Central locations were determined by means of the medial axis transform (see Amenta et al. 2001). Also known as 'skeletonization', this operation reduces a 3D object volume (such as the endocast of the bony labyrinth) to a set of connected lines (the 'skeleton'), where each line point represents a local centre of the object (see also Fig. S1). Most

Table 1 Sample list, protocol of data acquisition and EMBL genetic sequences used in the analyses.

Genus	Species	Family	Collection*	No.	Ears (L/R)	Vox size (μm)	Scanner	EMBL id sequence	Age
Lemurs									
Allocebus	*trichotis*	Cheirogaleidae	MNHN MO	2002-1	L/R	36	Scanco μCT80	AY441461	Adult
Cheirogaleus	*medius*	Cheirogaleidae	AIM-ZU	8128	L/R	74	Scanco μCT80	AY441458	Adult
Cheirogaleus	*major*	Cheirogaleidae	MNHN MO	2002_87	L/R	50	Scanco μCT80	AY441457	Adult
Phaner	*furcifer*	Cheirogaleidae	MNHN MO	1962-2712	L/R	36	Scanco μCT80	AY441456	Adult
Microcebus	*murinus*	Cheirogaleidae	AIM-ZU	5065-10	L/R	36	Scanco μCT80	AF285557	Adult
Microcebus	*murinus*	Cheirogaleidae	AIM-ZU	5065-12	L/R	36	Scanco μCT80	AF285557	Adult
Microcebus	*rufus*	Cheirogaleidae	MNHN MO	1882-1550	L/R	36	Scanco μCT80	AF285544	Adult
Mirza	*coquereli*	Cheirogaleidae	AIM-ZU	1869-198	L/R	36	Scanco μCT80	AY441462	Adult
Eulemur	*fulvus*	Lemuridae	MONTP	No n°	L/R	60	ESRF ID19	AF081048	Subadult
Eulemur	*mongoz*	Lemuridae	AIM-ZU	1214	L/R	74	Scanco μCT80	AF081051	Adult
Eulemur	*rubriventer*	Lemuridae	AIM-ZU	10599	L/R	74	Scanco μCT80	AF081052	Adult
Hapalemur	*griseus*	Lemuridae	AIM-ZU	5055	L/R	74	Scanco μCT80	AY441447	Adult
Indri	*indri*	Indriidae	AIM-ZU	AS-919	L/R	74	Scanco μCT80	AY441455	Adult
Avahi	*laniger*	Indriidae	AIM-ZU	1827	L/R	74	Scanco μCT80	AY441453	Adult
Avahi	*occidentalis*	Indriidae	AIM-ZU	13884	L/R	74	Scanco μCT80	AY441454	Adult
Daubentonia	*madagascariensis*	Daubentoniidae	MONTP	MO	L/R	60	ESRF ID19	AY441444	Adult
Daubentonia	*madagascariensis*	Daubentoniidae	AIM-ZU	AS-1843	L	74	Scanco μCT80	AY441444	Adult
Lemur	*catta*	Lemuridae	AIM-ZU	9601	L/R	74	Scanco μCT80	AF175953	Adult
Lepilemur	*dorsalis*	Lepilemuridae	MNHN MO	2002-6	L/R	50	Scanco μCT80	DQ108993	Adult
Lepilemur	*leucopus*	Lepilemuridae	AIM-ZU	5058	L/R	74	Scanco μCT80	DQ109007	Adult
Lepilemur	*mustelinus*	Lepilemuridae	MNHN MO	2002-3	L/R	50	Scanco μCT80	DQ109033	Adult
Lepilemur	*ruficaudatus*	Lepilemuridae	AIM-ZU	11054	L/R	74	Scanco μCT80	DQ109011	Adult
Lepilemur	*ruficaudatus*	Lepilemuridae	AIM-ZU	10614	L/R	74	Scanco μCT80	DQ109011	Adult
Propithecus	*diadema*	Indriidae	AIM-ZU	7255	L/R	74	Scanco μCT80	AY441452	Adult
Propithecus	*verreauxi*	Indriidae	AIM-ZU	AS-131	L/R	74	Scanco μCT80	AF285528	Adult
Varecia	*variegata*	Lemuridae	AIM-ZU	As 805	L/R	74	Scanco μCT80	AF081047	Adult
Galagos									
Euoticus	*elegantulus*	Galagidae	AIM-ZU	7712	L/R	45.71	ESRF ID17	AY441469	Adult
Galago	*alleni*	Galagidae	AIM-ZU	7925	L/R	45.71	ESRF ID17		Adult
Galago	*moholi*	Galagidae	MNHN MO	1885-196	L/R	36	Scanco μCT80	AF271410	Adult
Otolemur	*crassicaudatus*	Galagidae	AIM-ZU	1841	L/R	45.71	ESRF ID17	AY441465	Adult
Galagoides	*demidoff*	Galagidae	AIM-ZU	6535	L/R	45.71	ESRF ID17	AF271411	Adult
Otolemur	*garnetti*	Galagidae	AIM-ZU	AS926	L/R	45.71	ESRF ID17	AF271412	Adult
Galago	*senegalensis*	Galagidae	AIM-ZU	6591	L/R	45.71	ESRF ID17	AY441471	Adult
Lorises									
Arctocebus	*calabarensis*	Lorisidae	AIM-ZU	7730	L/R	98	EMPA	AY441474	Adult
Loris	*tardigradus*	Lorisidae	AIM-ZU	9950	L/R	45.71	ESRF ID17	AY441475	Adult

Table 1 Continued

Genus	Species	Family	Collection*	No.	Ears (L/R)	Vox size (μm)	Scanner	EMBL id sequence	Age
Nycticebus	*coucang*	Lorisidae	AIM-ZU	10586	L/R	74	Scanco μCT80	AY687889	Adult
Perodicticus	*potto*	Lorisidae	AIM-ZU	7425	L/R	60	ESRF ID17	AF271413	Adult
Pseudopotto	*martini*	Lorisidae	AIM-ZU	6698	L/R	50	Scanco μCT80		Adult
Anthropoids									
Aotus	*trivirgatus*	Cebidae	AIM-ZU	1775	L/R	45.71	ESRF ID17	DQ098873	Adult
Callithrix	*jacchus*	Cebidae	AIM-ZU	10168	L/R	36	Scanco μCT80	AF295586	Adult
Trachypithecus	*vetulus*	Cercopithecidae	AIM-ZU	10736	L/R	74	Scanco μCT80	AF295577	Adult
Semnopithecus	*entellus*	Cercopithecidae	AIM-ZU	12520	L/R	74	Scanco μCT80	AF012470	Subadult
Gorilla	*gorilla*	Hominoidae	AIM-ZU	5563	L/R	500*90*90	Med. scanner	D38114	Adult
Pan	*troglodytes*	Hominoidae	AIM-ZU	5717	L/R	500*90*90	Med. scanner	D38113	Adult
Tarsiers									
Tarsius	*bancanus*	Tarsiidae	AIM-ZU	PAL-44	L/R	36	Scanco μCT80	AB011077	Adult
Tarsius	sp.	Tarsiidae	AIM-ZU	1202	L/R	36	Scanco μCT80		Adult
Tarsius	*syrichta*	Tarsiidae	AIM-ZU	AS-1732	L/R	78	EMPA		Adult
Tarsius	*spectr*	Tarsiidae	AIM-ZU	AS-1821	L/R	36	Scanco μCT80		Adult
Fossils									
Palaeolemur	*betillei*	Adapidae	MHN BX	Bor-613	L/R	30	ESRF ID19		Adult
Adapis	sp.	Adapidae	MONTP	ACQ208	L	45.7	ESRF ID17		Adult
Adapis	sp.	Adapidae	MONTAU	MAPHQ 223	R	30	ESRF ID19		Adult
Adapis	sp.	Adapidae	MONTAU	MAPHQ 051	L	30	ESRF ID19		Adult
Adapis	sp.	Adapidae	MÜNCH	XV-1869-1530	L/R	30	ESRF ID19		Adult
Adapis	sp.	Adapidae	MÜNCH	XV-1869-2	L/R	30	ESRF ID19		Adult
Adapis	sp.	Adapidae	BASEL	QW1530	R	30	ESRF ID19		Adult
Adapis	sp.	Adapidae	BASEL	QW1	R	50	Scanco μCT80		Adult
Lepdatapis	sp.	Adapidae	MONTP	ACQ209	R	45.71	ESRF ID19		Adult
Non-primates									
Tupaia	*tana*	Tupaiidae	AIM-ZU	AS-1851	L/R	50	Scanco μCT80		Adult
Tupaia	*glis*	Tupaiidae	AIM-ZU	10591	L/R	36	Scanco μCT80	AY321641	Adult
Cynocephalus	*volens*	Cynocephalidae	AIM-ZU	AS-1904	L/R	50	Scanco μCT80	AB075974	Subadult
Galeopterus	*variegatus*	Cynocephalidae	MONTP	CCL01	L/R	30	ESRF ID19	AF460846	Adult

*AIM-ZU, Antropologisches Institut und Museum Zürich; MHN BX, Musée d'Histoire Naturelle de Bordeaux; MÜNCH, Museum und Institut für Palaeontologie München; MNHN MO, Muséum National d'Histoire Naturelle, Laboratoire Mammifères et Oiseaux, Paris; MONTAU, Museé d'Histoire Naturelle de Montauban; BASEL, Naturhistorisches Museum Basel; MONTP, Institut des Sciences de l'Evolution de Montpellier.

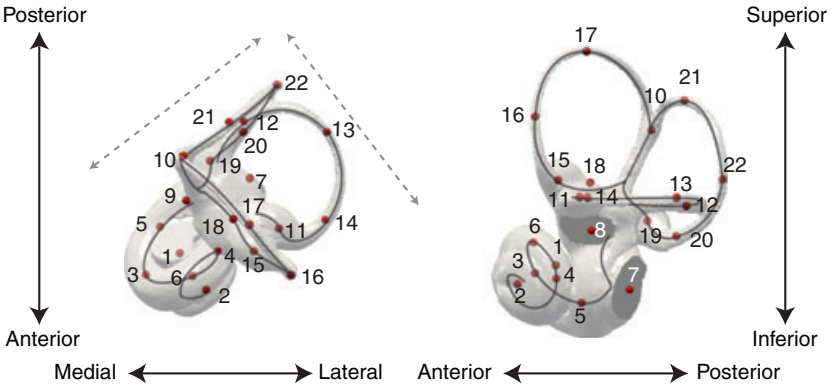

Fig. 1 Landmarks used for geometric morphometric analysis of the bony labyrinth (specimen: *Lepilemur ruficaudatus* AIM-11054). Grey arrows: anteromedial-to-posterolateral and anterolateral-to-posteromedial directions used to define landmark locations 3–4, 12–14, 16 and 22. The superior-to-inferior direction was used to define landmark locations 5–6, 17–18, 20–21 (see Table 1). Grey line: a simplified version of the medial axis.

Table 2 Landmarks.

N°	Name	Definition
1	Helix basis	Centre of the first turn of the cochlea (within the plane defined by the first turn of the cochlea)
2	Helix apex	Centre of the last turn of the cochlea (within the plane defined by the last turn of the cochlea)
3	Helix anteromedial	Anteromedial-most point at the centre of the lumen of the first turn of the cochlea
4	Helix posterolateral	Posterolateral-most point at the centre of the lumen of the first turn of the cochlea
5	Helix inferior	Inferior-most point at the centre of the lumen of the first turn of the cochlea
6	Helix superior	Superior-most point at the centre of the lumen of the first turn of the cochlea
7	Fenestra cochlea	Centre of the round window
8	Fenestra vestibuli	Centre of the oval window
9	Aquaeductus vestibuli	Opening of the vestibular aqueduct in the vestibular wall
10	Crus commune apex	Bifurcation point of the common crus
11	Canalis lateralis ampulla	Centre of the ampulla of the lateral semicircular canal
12	Canalis lateralis posteromedial	Posteromedial-most point at the centre of the lumen of the lateral semicircular canal
13	Canalis lateralis posterolateral	Posterolateral-most point at the centre of the lumen of the lateral semicircular canal
14	Canalis lateralis anterolateral	Anterolateral-most point at the centre of the lumen of the lateral semicircular canal
15	Canalis anterior ampulla	Centre of the ampulla of the anterior semicircular canal
16	Canalis anterior anterolateral	Anterolateral-most point at the centre of the lumen of the anterior semicircular canal
17	Canalis anterior superior	Superior-most point at the centre of the lumen of the anterior semicircular canal
18	Canalis anterior inferior	Inferior-most point of the vestibular wall lying in the anterior semicircular canal plane
19	Canalis posterior ampulla	Centre of the ampulla of the posterior semicircular canal
20	Canalis posterior inferior	Inferior-most point at the centre of the lumen of the posterior semicircular canal
21	Canalis posterior superior	Superior-most point at the centre of the lumen of the posterior semicircular canal
22	Canalis posterior posterolateral	Posterolateral-most point at the centre of the lumen of the posterior semicircular canal

landmark locations were defined relative to the three main axes of the labyrinth, which, using cranial anatomical directions, are along anteromedial-to-posterolateral, anterolateral-to-posteromedial, and superior-to-inferior lines (see Fig. 1). Additional landmark locations were defined at centres of anatomical structures (the ampullae of the semicircular canals, the basis and vertex of the cochlear helix, and the oval and round windows), and at the bifurcation of the common crus (see Fig. 1 and Table 2 for details).

The form of the cranium was quantified with 51 landmarks (26 facial, 13 neurocranial, 12 basicranial; Fig. S2), defined at the intersection of bone sutures, the centre of foramina and maxima of curvature.

Data analysis

Using generalized least-squares fitting (Rohlf, 1990) and principal components analysis (PCA) of shape (Dryden & Mardia, 1998), the form of each specimen's landmark configuration was represented by its centroid size *S*, and by its multidimensional shape vector *v* in linearized Procrustes shape space. Analysis and visualization of patterns of shape variation were performed with the interactive software package MorphoTools (Specht, 2007; Specht et al. 2007; Lebrun, 2008). Secondly, to assess whether the labyrinthine shape is a good taxonomical marker, we used linear discriminant analysis to compute a function that best discriminates among the families. Then the posterior prob-

abilities to belong to the predefined groups were assessed based on each specimen's squared Mahalanobis distance to each family's centroid. We used R 2.7.0 (Ihaka & Gentelman, 1996) to perform this analysis.

Phenetic distances between taxa were computed as the Procrustes distances between taxon-specific mean shapes for the following landmark configurations: inner ear, entire cranium, face, basicranium, neurocranium. Size-corrected shape distances were obtained as follows. Regressions of Procrustes coordinates against the logarithm of centroid size were computed for all extant strepsirrhine families (except for the Daubentoniidae, as they are mono-specific), yielding family-specific allometric shape vectors (ASV_s). The ASV_s represent directions in shape space which characterize family-specific allometric patterns of shape variation. A common allometric shape vector (ASV_c), obtained as the mean of all the strepsirrhine ASV_s, provided a direction in shape space that minimizes potential divergence in allometric patterns across extant families (see Ponce de León & Zollikofer, 2006, for further details concerning this methodology). ASV_c was then used to decompose each specimen's shape into size-related (v_s) and size-independent (v_i) components. The latter component was used to calculate between-taxon size-corrected distances: assuming that ASV_c characterized common allometric patterns well for the whole sample, the fossil Adapinae, Anthropoidea, *Tarsius*, Scandentia and Dermoptera were also projected onto ASV_c to retrieve the size-independent component of labyrinthine shape.

Genetic distances between taxa were estimated with molecular data (mitochondrial cytochrome *b* sequences; EMBL access IDs and lists of species are provided in Table 1). Adopting the methodology of Yoder et al. (1996), we computed molecular distances with PHYLIP (Felsenstein, 1989), using Kimura two-parameter (Kimura, 1980) corrections incorporating a 10 : 1 transition/transversion ratio.

Correlations between molecular and phenetic distances were evaluated using linear regression. Calculations were performed for species-wise distances and for average intra- and inter-family distances (Fig. 2, Table 3). Size-corrected labyrinthine shape (which yielded the highest correlation when strepsirrhine specimens were considered; see Results) was used to calculate a phenetic distance matrix. Taxa were clustered using the NJ (neighbour joining) and UPGMA (unweighted pair-group method using an arithmetic average) procedures (Fig. 3). A landmark-based random sampling procedure, as described in Lockwood et al. (2004), was executed 1000 times. The associated consensus NJ and UPGMA trees were computed using PHYLIP (Felsenstein, 1989).

Results

Graphing phenetic between-taxon distances vs. molecular between-taxon distances shows the highest correlations for size-corrected labyrinthine shape when strepsirrhine taxa are considered alone, while correlations for cranial, basicranial and facial morphology are lower (Fig. 2, Table 3). When haplorhines and non-primate taxa are included in the analysis, phenetic distances and molecular distances correlate better for cranial morphology than for inner ear morphology (Fig. 2, Table 3). Figure 2B shows that, considering the large genetic distance between strepsirrhine and anthropoid taxa, the labyrinthine morphological distances tend to be relatively small (see Fig. 2B).

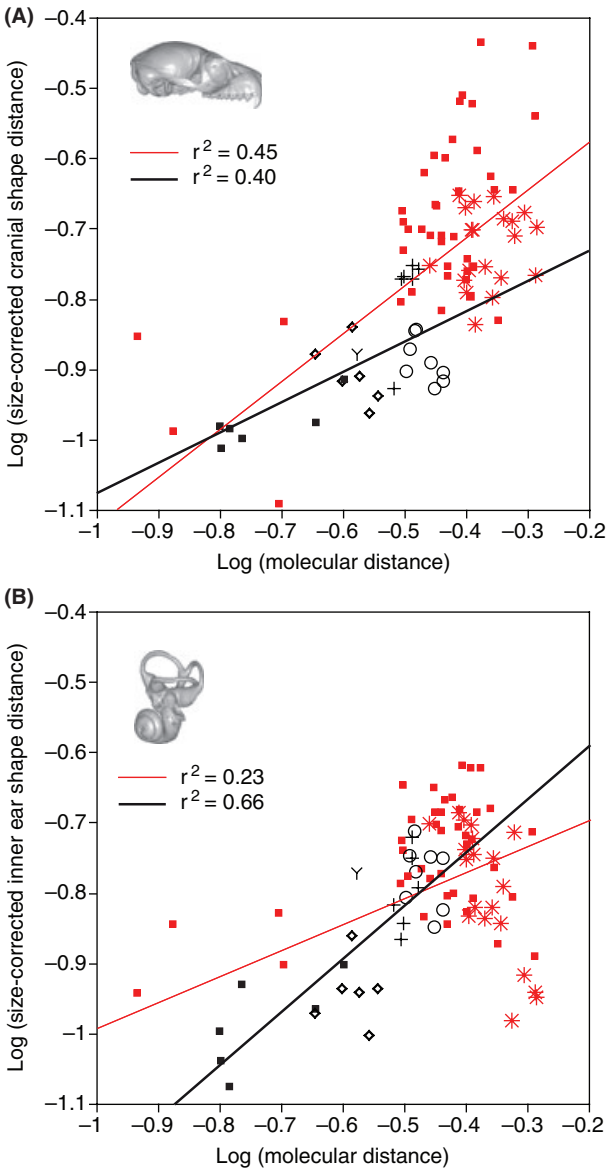

Fig. 2 Correlations between molecular distances and corresponding phenetic distances. (A) Graph of size-corrected cranial shape distance vs. molecular distance. (B) Graph of size-corrected bony labyrinth shape distance vs. molecular distance. Black squares: strepsirrhine intra-familial distances; Diamonds: lemuroid inter-familial distances (Cheirogaleidae, Lepilemuridae, Lemuridae and Indriidae). Y: lorisiform inter-familial distance (Lorisidae–Galagidae). Open circles: lemuriform–lorisiform inter-familial distances. Crosses: distances between Daubentonia and Lemuroidea families. Stars: inter-familial distances between strepsirrhines and anthropoids. Red squares: other inter- and intra-familial distances involving at least one non-strepsirrhine taxon. Black regression lines are for strepsirrhine taxa only, red regression lines for all analyzed taxa (see Table S2 for regression summaries).

To assess the diagnostic value of inner ear morphology at the family level, we performed a linear discriminant analysis on the full set of PC scores of the PCA of shape. All the spec-

Table 3 Correlations between log-transformed phenetic and molecular distances.

Phenetic (shape) distance	r_1^2	P_1	df_1	r_2^2	P_2	df_2	r_3^2	P_3	df_3	r_4^2	P_4	df_4
Inner ear	0.35	< 0.0001	87	0.65	< 0.0001	26	0.30	< 0.0001	902	0.35	< 0.0001	527
Size-corrected inner ear	0.23	< 0.0001	87	0.66	< 0.0001	26	0.23	< 0.0001	902	0.36	< 0.0001	527
Cranium	0.46	< 0.0001	87	0.39	0.0005	26	0.37	< 0.0001	902	0.15	< 0.0001	527
Size-corrected cranium	0.45	< 0.0001	87	0.40	0.0004	26	0.44	< 0.0001	902	0.14	< 0.0001	527
Basicranium	0.41	< 0.0001	87	0.33	0.0018	26	0.45	< 0.0001	902	0.14	< 0.0001	527
Size-corrected basicranium	0.39	< 0.0001	87	0.34	0.0013	26	0.37	< 0.0001	902	0.14	< 0.0001	527
Face	0.53	< 0.0001	87	0.37	0.0008	26	0.45	< 0.0001	902	0.17	< 0.0001	527
Size-corrected face	0.54	< 0.0001	87	0.39	0.0005	26	0.44	< 0.0001	902	0.16	< 0.0001	527
Neurocranium	0.25	< 0.0001	87	0.07	0.17	26	0.21	< 0.0001	902	0.03	0.001	527
Size-corrected neurocranium	0.21	< 0.0001	87	0.05	0.27	26	0.20	< 0.0001	902	0.02	< 0.0001	527

r_1, P_1, df_1: regressions at the family level, including all pairs of families involving non-strepsirrhine taxa also. r_2, P_2, df_2: regressions at the family level, involving strepsirrhine taxa only. r_3, P_3, df_3: regressions at the species level, including all pairs of species involving non-strepsirrhine taxa. r_4, P_4, df_4: regressions at the species level, involving strepsirrhine taxa only.

imens were correctly classified *a posteriori* to their original family, with posterior probabilities ranging between 0.94 and 1.0. This result supports the hypothesis that the morphology of the inner ear, as quantified by the configuration of 22 three-dimensional landmarks, serves as a reliable taxonomic marker at the family level.

The potential and limitations of phyletic analyses based on inner ear morphology are illustrated in Fig. 3. Phenetic consensus trees correctly retrieved the Lorisiformes (Galagidae and Lorisidae) and the Lemuroidea clades (Cheirogaleidae, Lepilemuridae, Lemuridae and Indriidae) (Fig. 3A,B). However, the relative position of *Daubentonia*, Adapinae, *Tarsius*, Anthropoidea and the non-primate Scandentia and Dermoptera do not reflect the current view of primate phylogeny. *Daubentonia*, the most derived extant Malagasy primate genus, does not branch at the base of the Lemuroidea clade.

Interestingly, Adapinae and *Daubentonia* share labyrinthine features: their lateral semicircular canal is relatively small (though not as small as that of lorisids), and the ampullar segment of the posterior canal is fused with the posterior-most segment of the lateral canal (Fig. 4). Also, *Daubentonia* has a large cochlea relative to the size of the labyrinth, as well as an unusually long common crus, which are features contrasting with all other extant lemurs.

Visualizing patterns of labyrinthine shape variation in morphospace and in physical space permits characterization of size allometry and of taxon-specific morphologies (Fig. 5). Large inner ears are characterized by a high position of the posterior semicircular canal, a long common crus, large superior but small lateral canals, and a small, laterally oriented cochlea. Figure 5 also shows a clear separation between lemuriform and lorisiform labyrinthine morphologies. Lemuriform labyrinths are characterized by round lateral canals, posterior canals located in a low position relative to the lateral canals, long common crura, and cochleae that usually exhibit between 2 and 2.5 turns, whereas lorisiform labyrinths exhibit oval lateral canals, short common crura, and cochleae which have a wide first turn (Fig. 5) and tend to exhibit more than 2.5 turns. The labyrinthine morphology of Adapinae is close to that of the Malagasy lemurs. *Tarsius* labyrinths occupy an isolated position in shape space; they are characterized by large and round lateral semicircular canals (Matano et al. 1986), and relatively small superior and posterior canals. Anthropoid labyrinths occupy an intermediate position between the labyrinths of *Tarsius* and those of Cheirogaleidae. Among non-primates, *Cynocephalus* exhibits a labyrinthine shape that is close to that of Lemuriformes and Adapinae, whereas *Galeopterus* exhibits relatively larger lateral semicircular canals and smaller superior canals. The labyrinths of *Tupaia tana* and *Tupaia glis* occupy an isolated position in shape space. Their morphology differs substantially from that of primates; most notably, the superior semicircular canal is curved, and the cochlea exhibits three turns (Fig. 6).

Discussion

Our data show that labyrinthine phenetic distances between strepsirrhine taxa correlate well with genetic between-taxon distances evaluated from neutral molecular markers. Likewise, phyletic trees evaluated from labyrinthine shape exhibit partial congruence with gene-based phyletic trees, notably regarding the topology of the lorisiform and lemuriform subtrees. This congruence indicates that the inner ear – while being a functionally highly constrained structure – contains a strong signal of neutral evolution (Lande, 1976; Lynch, 1990).

Evolutionary change in the morphology of the bony labyrinth might thus be described with a random walk model (also sometimes called Brownian motion model; see Pagel, 1999), which postulates random phenotypic dispersal in morphospace over evolutionary time. However, the observed patterns of random dispersal do not necessarily

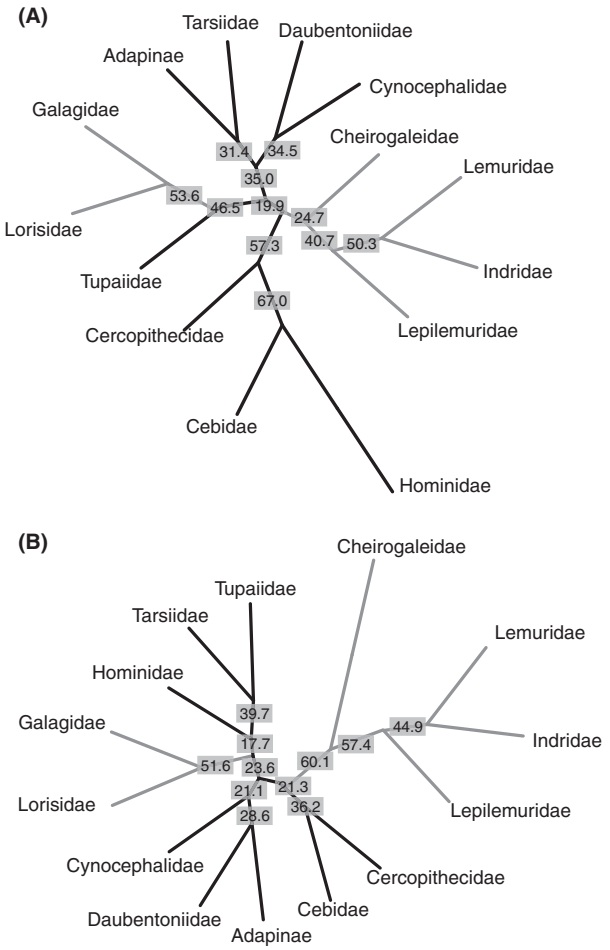

Fig. 3 Phenetic trees based on inner ear morphology (average labyrinthine shape of taxa). (A) NJ tree reflecting bony labyrinth morphological affinities (size-corrected shape distances) between strepsirrhine families, fossil Adapinae, *Tarsius*, anthropoids, Scandentia and Dermoptera. (B) UPGMA tree reflecting bony labyrinth morphological affinities (size-corrected shape distances) between strepsirrhine families, fossil Adapinae, *Tarsius*, anthropoids, Scandentia and Dermoptera. Bootstrap values for 1000 resamplings are given at each node. Lemuroidea families (Cheirogaleidae, Lepilemuridae, Lemuridae and Indriidae) are nested together in both trees, as well as the Lorisiformes (Galagidae and Lorisidae).

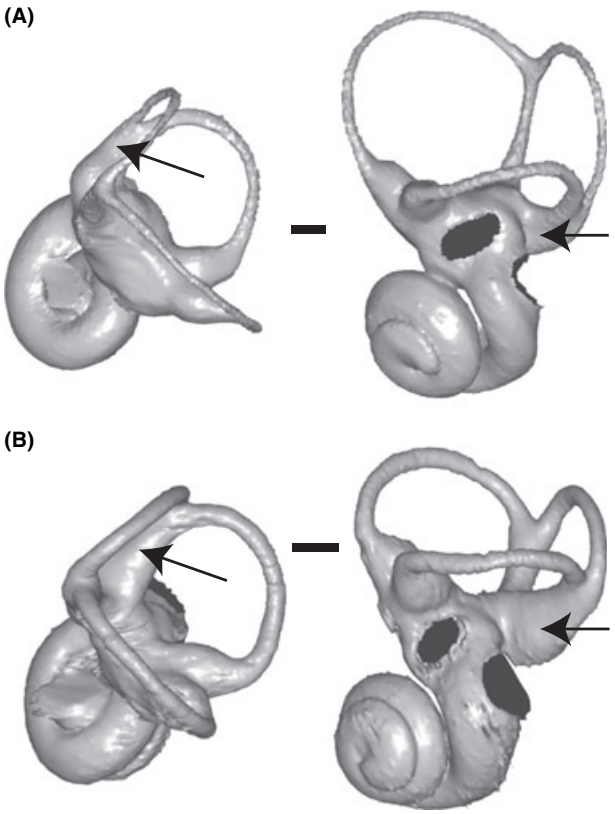

Fig. 4 Left bony labyrinth of *Daubentonia madagascariensis* (A) and *Palaeolemur betillei* (B). Labyrinths are oriented in superior (left) and lateral (right) views (by convention, the lateral semicircular canal is positioned horizontally). Arrows: in both species, the ampullar part of the posterior canal is fused with the medial part of the lateral canal. Specimens: AIM-ZU AS-1843 (*Daubentonia*) and Bor-613 (*Palaeolemur*). Scale bar: 1 mm.

imply an underlying random process, as they may result from the combined effects of various, and possibly conflicting, functional, adaptive and developmental constraints shaping labyrinthine architecture. In any case, given a random walk-like pattern of morphological evolution, geometric morphometric analysis is a tool well suited to elucidate character correlation in complex three-dimensional structures, to identify independent characters, to define character states, and to infer character state polarity. Assuming random walk-like phenotypic evolution in morphospace, average shapes calculated for each node of the phyletic tree give an estimate of inner ear shapes of the respective last common ancestors (LCAs) (Rohlf, 1998; Wiley et al. 2005). Following this logic, the clear division between lorisiform bony labyrinth morphologies, on the one hand, and those of Malagasy primates and adapines on the other, support the hypothesis that the lorisiform condition is derived, whereas that of the Malagasy primates and adapines is closer to the inferred primitive state, as represented by the sample mean shape (see Fig. S3). The notion that lorisiform labyrinthine morphology is derived stands in contrast to the view that lorisiforms as well as the lemuriform family of cheirogaleids exhibit a primitive basicranial morphology (Charles-Dominique & Martin, 1970). In the light of the evidence presented here, it is likely that basicranial similarities between lorisiforms and cheirogaleids result from size allometry and convergence.

Following the same logic of random walk-like phenotypic evolution, the inner ear morphology of Adapinae appears to be close to that inferred for basal Lemuriformes. This supports the hypothesis that Adapiformes are strepsirrhines (Kay et al. 1997; Yoder, 1997; Godinot, 1998; Rasmussen & Nekaris, 1998; Marivaux et al. 2001; Seiffert et al. 2003, 2009; Seiffert, 2005). Furthermore, the absence of similari-

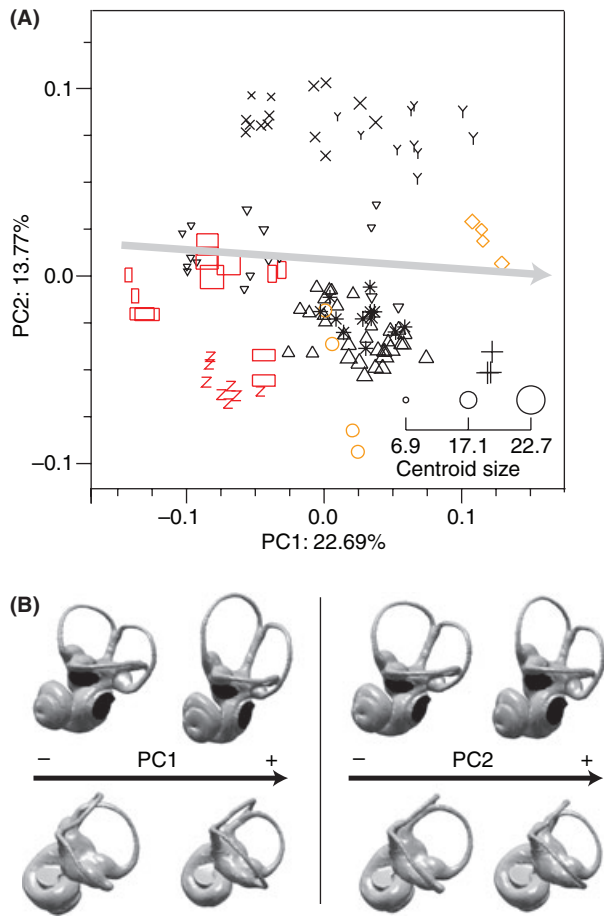

Fig. 5 Principal components analysis (PCA) of labyrinthine shape variation. (A) Graphing the first two components of shape space, PC1 and PC2, shows a common pattern of size-related shape variation (grey arrow approximately parallel to PC1), and major differences in shape between Malagasy primates and lorisiform primates (along PC2). Downward-pointing triangles: Cheirogaleidea; upward-pointing triangles: Lemuroidea; +: Daubentoniidae; X: Galagidae; Y: Lorisidae; stars: Adapinae; Z: Tarsiidae; Red vertical rectangles: Cebidae; Red horizontal rectangles: Cercopithecidae; Red squares: Hominidae; Orange diamonds: Scandentia; Orange circles: Dermoptera. (B) Patterns of labyrinthine shape variation associated with PC1 and PC2, respectively.

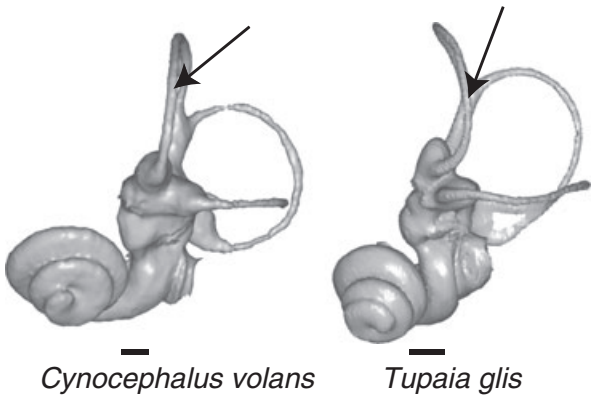

Fig. 6 Left bony labyrinths of *Cynocephalus volans* and *Tupaia tana*. Arrows: *Cynocephalus*, as well as extant primates, exhibits a straight superior canal, whereas *Tupaia* exhibits a curved superior canal. Specimens: AIM-ZU AS-1904 (*Cynocephalus*) and AIM-ZU 10591 (*Tupaia*). Scale bar: 1 mm.

ties between the bony labyrinths of Adapinae and anthropoids argues against the recently resurrected hypothesis that Adapiformes are linked with haplorhines, and in particular with anthropoids (Franzen et al. 2009; see also Gingerich, 1973; Rasmussen, 1990; Simons & Rasmussen, 1989).

Using molecular clock arguments, Yoder & Yang (2004) proposed that the evolutionary diversification of the Malagasy primates started in the Palaeocene, 62–65 Mya ago, and a similarly old divergence date might be true for the adapines. This implies that the inner ear morphology in these two groups is highly conserved and reflects the morphology of a Cretaceous or early Palaeocene LCA of strepsirrhines (Martin, 1993; Gingerich & Uhen, 1994; Tavaré et al. 2002) (see Fig. S3). Whereas cladistic analyses of cranial and postcranial morphology typically place the Adapinae at a basal position relatively to all extant strepsirrhine primates (Marivaux et al. 2001; Seiffert et al. 2003), labyrinthine evidence situates them together with *Tarsius* (Fig. 3A), or close to *Daubentonia* (Fig. 3B). These tree topologies might be an effect of the derived labyrinthine morphology of the lorisiforms, which occupy an isolated position in shape space. Also, *Daubentonia* does not appear at the expected basal position (Yoder et al. 1996; Roos et al. 2004) of the Malagasy primate clade. This placement might result from the unique combination of plesiomorphic and apomorphic features in the labyrinth of *Daubentonia madagascariensis*.

As mentioned, *Daubentonia* shares with the adapines partial fusion of the lateral and posterior semicircular canals (see Fig. 4). This condition occurs in a large number of non-primate mammal groups (including eutherians, marsupials and monotremes: see Hyrtl, 1845; Gray, 1907, 1908; Schmelzle et al. 2007; Denker, 1899). Fusion results from the low position of the lateral relative to the posterior canal (Hyrtl, 1845), and it only involves the bony cavities, not the functionally relevant endolymphatic ducts (Gray, 1907; p. 88). In our sample, fusion was observed in all specimens of Adapinae (n = 9) and *Daubentonia* (n = 2), but it was also found in one specimen of *Tarsius* sp. (AIM-ZU AS-1202). Furthermore, this condition occurs in *T. glis* and *Tupaia minor* (F. Spoor, pers. comm.), which suggests that fusion may not be a consistent feature within species. As a cautious interpretation of this evidence, we suggest that a low position of the posterior semicircular canal – often resulting in fusion with the ampullar segment of the lateral canal – represents a symplesiomorphic character still present in Adapinae and *Daubentonia*, but no longer present in other strepsirrhines. On the other hand, the labyrinth of *Daubentonia* also

Table 4 Shape and size variance of the inner ear morphology within each extant strepsirrhine primate families and in fossil Adapinae.

	Shape variance	df	Size variance	df	Mean centroid size	Size coefficient of variation
Galagidae	1.18*10-4	767	2.05	13	12.10	0.169
Lorisidae	1.55*10-4	531	1.93	9	12.82	0.151
Cheirogaleidae	1.80*10-4	885	1.41	15	9.93	0.141
Daubentoniidae	5.6*10-5	118	0.03	2	17.83	0.002
Indriidae	1.35*10-4	531	4.64	9	16.27	0.285
Lemuridae	9.35*10-5	649	0.54	11	15.50	0.035
Lepilemuridae	1.02*10-4	531	0.13	9	13.88	0.009
Adapinae	9.67*10-5	649	0.45	11	13.06	0.035

exhibits various autapomorphic features, such as a large cochlea relative to the size of the semi-circular canal system, and a long common crus (Fig. 4).

What is the relationship between locomotor and phylogenetic signals conveyed by the morphology of the bony labyrinth of strepsirrhines? Within lorisiforms, conspicuous differences in locomotor behaviour between the slow-moving lorises and the highly agile galagos are clearly associated with differences in lateral semicircular canal size (Matano et al. 1985; Spoor & Zonneveld, 1998; Walker et al. 2008) (see also Fig. S4). Our geometric morphometric analyses demonstrate that the locomotor signal separating these two groups is clearly discernible from the phylogenetic signal that characterizes the derived inner ear morphology of all lorisiforms and separates them from all Malagasy primates, irrespective of locomotor behaviour (Figs 3 and 5). Within Malagasy primates, the indriids (vertical clingers and leapers) and the lemurids (quadrupedalists) exhibit largely similar labyrinthine morphologies, despite wide variability in locomotor behaviour. Likewise, the adapines, which are thought to have exhibited a wide spectrum of locomotor specializations (Bacon & Godinot, 1998), exhibit little labyrinthine shape variability (see Table 4).

Our analyses showed that, for strepsirrhine taxa, genetic distances correlate better with labyrinthine phenetic distances than with cranial phenetic distances. However, when anthropoid taxa are included, this situation is reversed (see Fig. 2B and Table 3). Figure 2 indicates that, with increasing genetic distance, cranial phenetic distances increase, whereas labyrinthine phenetic distances appear to attain an upper limit. There are several non-exclusive interpretations of these findings. One possibility is that variation of the labyrinthine morphology occurs within a comparatively small region of morphospace, which is confined by general functional and/or developmental constraints. Another interpretation is that labyrinthine morphologies of strepsirrhines and anthropoids converge in some respects, possibly reflecting specific functional constraints. These results call for an extended analysis of the phylogenetic and functional correlates of strepsirrhine and anthropoid labyrinthine morphology.

Concluding remarks

Our results demonstrate that geometric morphometric methods provide a suitable means to distinguish between locomotor, allometric and phylogenetic components of labyrinthine shape variability. Especially in strepsirrhine primates, the phylogenetic signal conveyed by the morphology of the inner ear appears to be strong: labyrinthine morphology of the inner ear is surprisingly conserved through evolutionary time and is well correlated with neutral molecular markers. Analyzing the combined phylogenetic and functional signals contained in the three-dimensional shape of the bony labyrinth may provide new insights into the evolutionary history and functional specialization not only of the strepsirrhines, but of living and extinct mammalian taxa in general.

Author contributions

R. Lebrun wrote the manuscript, performed the research and wrote analytical tools. Marcia P. de León designed the research and revised the article. P. Tafforeau acquired data and revised the article. Christoph Zollikofer wrote the manuscript and designed the research.

Acknowledgements

We thank Jean-Jacques Jaeger for helpful comments. We are grateful to the curators for giving access to fossil and extant specimens: Edmée Ladier (Musée d'Histoire Naturelle de Montauban), Nathalie Mémoire (Musée d'Histoire Naturelle de Bordeaux), Kurt Heissig (Museum und Institut für Paläontologie, München), Burkart Engesser and Arne Ziems (Naturhistorisches Museum Basel), Jacques Cuisin (Collection des Mammifères et des Oiseaux, Museum d'Histoire Naturelle de Paris), Monique Vianey-Liaud, Bernard Marandat and Suzanne Jiquel (Institut des Sciences de l'Evolution de Montpellier). We thank the staff of beamlines ID19 and ID17 (ESRF), and Peter Wyss (EMPA) for help with microtomography. Special thanks to Matthias Specht for collaborative implementation of MorphoTools. Thanks to Pierre-Henri Fabre for advice with molecular data and to Laurent Marivaux for advice concerning the manuscript.

References

Amenta N, Choi S, Kolluri R (2001) *The Power Crust*. Proceedings of the Sixth ACM Symposium on Solid Modeling and Applications, pp. 249–260. Ann Arbor: Association for Computing Machinery.

Bacon A-M, Godinot M (1998) Analyse morphofonctionnelle des fémurs et des tibias des '*Adapis*' du Quercy: mise en évidence de cinq types morphologiques. *Folia Primatol* **69**, 1–21.

Betti L, Balloux F, Amos W, et al. (2009) Ancient demography, not climate, explains within-population phenotypic diversity in humans. *Proc R Soc Edinb Biol* **276**, 809–814.

Bradley BJ (2008) Reconstructing phylogenies and phenotypes: a molecular view of human evolution. *J Anat* **212**, 337–353.

Charles-Dominique P, Martin RD (1970) Evolution of lorises and lemurs. *Nature* **227**, 257–260.

Dagosto M (1983) Postcranium of *Adapis parisiensis* and *Leptadapis magnus* (Adapiformes, Primates). Adaptational and phylogenetic significance. *Folia Primatol* **41**, 49–101.

Dagosto M (1993) Postcranial anatomy and locomotor behavior in Eocene primates. In: *Postcranial Adaptation in Nonhuman Primates* (ed Gebo DL), pp. 199–219. DeKalb: Northern Illinois University Press.

Denker A (1899) *Vergleichend-anatomische Untersuchungen über das Gehörorgan der Säugethiere nach Corrosionspräparaten und Knochenschnitten*. Leipzig: Von Veit and Co.

Dryden IL, Mardia KV (1998) *Statistical Shape Analysis*. Chichester: John Wiley & Sons.

Felsenstein J (1989) PHYLIP - Phylogeny Inference Package (Version 3.2). *Cladistics* **5**, 164–166.

Fox RC, Meng J (1997) An X-radiographic and SEM study of the osseous inner ear of multituberculates and monotremes (Mammalia): implications for mammalian phylogeny and evolution of hearing. *Zool J Linn Soc* **121**, 249–291.

Franzen JL, Gingerich PD, Habersetzer J, et al. (2009) Complete primate skeleton from the Middle Eocene of Messel in Germany: morphology and paleobiology. *PLoS ONE* **4**, e5723.

Gebo DL (1983) Foot morphology and locomotor adaptation in Eocene primates. *Folia Primatol* **50**, 3–41.

Gibbs S, Collard M, Wood B (2002) Soft-tissue anatomy of the extant hominoids: a review and phylogenetic analysis. *J Anat* **200**, 3–49.

Gingerich PD (1973) Anatomy of the temporal bone in the Oligocene anthropoid *Apidium* and the origin of Anthropoidea. *Folia Primatol* **19**, 329–337.

Gingerich PD, Uhen MD (1994) Time of origin of primates. *J Human Evol* **27**, 443–445.

Godinot M (1998) A summary of adapiform systematics and phylogeny. *Folia Primatol* **69**, 218–249.

González-Jose R, Escapa I, Neves WA, et al. (2008) Cladistic analysis of continuous modularized traits provides phylogenetic signals in *Homo* evolution. *Nature* **453**, 775–779.

Gray AA (1907) *The Labyrinth of Animals, Vol. 1*. London: Churchill.

Gray AA (1908) *The Labyrinth of Animals, Vol. 2*. London: Churchill.

Harvati K, Weaver TD (2006) Human cranial anatomy and the differential preservation of population history and climate signatures. *Anat Rec A Discov Mol Cell Evol Biol* **288A**, 1225–1233.

Hublin J-J, Spoor F, Braun M, et al. (1996) A late Neanderthal from Arcy-sur-Cure associated with upper palaeolithic artefacts. *Nature* **381**, 224–226.

Hyrtl J (1845) *Vergleichend-anatomische Untersuchungen über das innere Gehörorgan des Menschen und der Säugethiere*. Prague: Verlag von Friedrich Ehrlich.

Ihaka R, Gentelman R (1996) R: a language for data analysis and graphics. *J Comput Graph Stat* **5**, 299–314.

Janecka JE, Miller W, Pringle TH, et al. (2007) Molecular and genomic data identify the closest living relative of primates. *Science* **318**, 792–794.

Kay RF, Ross CF, Williams BA (1997) Anthropoid origins. *Science* **275**, 797–803.

Ketten DR (1992) The cetacean ear: form, frequency, and evolution. In: *Marine Mammal Sensory Systems* (eds Thomas JA, Kastelein R, Supin A), pp. 56–69. New York: Plenum Press.

Kimura M (1980) A simple method for estimating evolutionary rates of base substitutions through comparative studies of nucleotide sequences. *J Mol Evol* **16**, 111–120.

Lande R (1976) Natural selection and random genetic drift in phenotypic evolution. *Evolution* **30**, 314–334.

Lebrun R (2008) Evolution and development of the strepsirrhine primate skull. Ph.D. Dissertation, University Montpellier II, University of Zürich, Montpellier, Zürich.

Lockwood CA, Kimbel WH, Lynch JM (2004) Morphometrics and hominoid phylogeny: support for a chimpanzee–human clade and differentiation among great ape subspecies. *Proc Natl Acad Sci U S A* **101**, 4356–4360.

Lynch M (1990) The rate of morphological evolution in mammals from the standpoint of neutral expectation. *Am Nat* **136**, 727–741.

Madsen O, Scally M, Douady CJ, et al. (2001) Parallel adaptive radiations in two major clades of placental mammals. *Nature* **409**, 610–614.

Manica A, Amos W, Balloux F, et al. (2007) The effect of ancient population bottlenecks on human phenotypic variation. *Nature* **448**, 346–349.

Manoussaki D, Chadwick RS, Ketten DR, et al. (2008) The influence of cochlear shape on low-frequency hearing. *Proc Natl Acad Sci U S A* **105**, 6162–6166.

Marivaux L, Welcome J-L, Antoine PO, et al. (2001) A fossil lemur from the Oligocene of Pakistan. *Science* **294**, 587–591.

Martin RD (1972) Adaptative radiation and behavior of the malagasy lemurs. *Philos Trans R Soc Lond B Biol Sci* **264**, 295–352.

Martin RD (1993) Primate origins: plugging the gaps. *Nature* **363**, 223–234.

Matano S, Kubo T, Günther M (1985) Semicircular canal organ in three primate species and behavioural correlations. *Fortschr Zool* **30**, 677–680.

Matano S, Kubo T, Matsunaga T, et al. (1986) On size of the semicircular canals organ in *Tarsius bancanus*. In: *Current Perspectives in Primate Biology* (eds Taub DM, King FA), pp. 122–129. New York: Van Nostrand Reinhold.

Meng J, Fox RC (1995) Osseous inner ear structures and hearing in early marsupials and placentals. *Zool J Linn Soc* **115**, 47–71.

Pagel M (1999) Inferring the historical patterns of biological evolution. *Nature* **401**, 877–884.

Pastorini J, Martin RD, Ehresmann P, et al. (2001) Molecular phylogeny of the lemur family cheirogaleidae (primates) based on mitochondrial DNA sequences. *Mol Phylogenet Evol* **19**, 45–56.

Pastorini J, Forstner M, Martin RD (2002) Phylogenetic relationships of gentle lemurs. *Evol Anthropol* **11**(suppl 1), 150–154.

Pastorini J, Thalmann U, Martin RD (2003) A molecular approach to comparative phylogeography of extant Malagasy lemurs. *Proc Natl Acad Sci U S A* **100**, 5879–5884.

Pilbeam D (1997) Research on Miocene hominoids and hominid origins: the last three decades. In: *Function, Phylogeny, and Fossils: Miocene Hominoid Evolution and Adaptations* (eds Begun DR, Ward CV, Rose MD), pp. 13–28. New York: Plenum.

Ponce de León MS, Zollikofer CPE (2006) Neanderthals and modern humans – chimps and bonobos: similarities and differences in development and evolution. In: *Neanderthals Revisited: New Approaches and Perspectives* (eds Harvati K, Harrison T), pp. 71–90. Dordrecht: Springer.

Poux C, Douzery EJP (2004) Primate phylogeny, evolutionary rate variations, and divergence times: a contribution from the nuclear gene IRBP. *Am J Phys Anthropol* **124**, 1–16.

Rasmussen DT (1990) The phylogenetic position of *Mahgarita stevensi*: protoanthropoid or lemuroid? *Int J Primatol* **11**, 439–469.

Rasmussen DT, Nekaris KA (1998) Evolutionary history of lorisiform primates. *Folia Primatol* **69**, 250–285.

Rohlf FJ (1990) Rotational fit (Procrustes) method. In: *Proceedings of the Michigan Morphometrics Workshop* (eds Rohlf FJ, Bookstein FL), pp. 227–236. Ann Arbor: The University of Michigan Museum of Zoology.

Rohlf FJ (1998) On applications of geometric morphometrics to studies of ontogeny and phylogeny. *Syst Biol* **47**, 147–158.

Romero I, Manica A, Goudet J, et al. (2009) How accurate is the current picture of human genetic variation? *Heredity* **102**, 120–126.

Roos C, Schmitz J, Zischler H (2004) Primate jumping genes elucidate strepsirrhine phylogeny. *Proc Natl Acad Sci U S A* **101**, 10650–10654.

Roseman CC, Weaver TD (2007) Molecules versus morphology? Not for the human cranium. *BioEssays* **29**, 1185–1188.

Rosowski JJ, Graybeal A (1991) What did Morganucodon hear? *Zool J Linn Soc* **101**, 131–168.

Schmelzle T, Sánchez-Villagra MR, Maier W (2007) Vestibular labyrinth diversity in diprotodontian marsupial mammals. *Mammal Study* **32**, 83–97.

Seiffert ER (2005) Additional remains of *Wadilemur elegans*, a primitive stem galagid from the late Eocene of Egypt. *Proc Natl Acad Sci U S A* **102**, 11396–11401.

Seiffert ER, Simons EL, Attia Y (2003) Fossil evidence for an ancient divergence of lorises and galagos. *Nature* **422**, 421–424.

Seiffert ER, Perry JMG, Simons EL, et al. (2009) Convergent evolution of anthropoid-like adaptations in Eocene adapiform primates. *Nature* **461**, 1118–1122.

Silcox MT, Bloch JI, Boyer DM, et al. (2009) Semicircular canal system in early primates. *J Human Evol* **56**, 315–327.

Simons EL, Rasmussen DT (1989) Cranial morphology of *Aegyptopithecus* and *Tarsius* and the question of the tarsier-Anthropoidean clade. *Am J Phys Anthropol* **79**, 1–23.

Smith HF, Terhune CE, Lockwood CA (2007) Genetic, geographic, and environmental correlates of human temporal bone variation. *Am J Phys Anthropol* **134**, 312–322.

Specht M (2007) Spherical surface parameterization and its application to geometric morphometric analysis of the braincase. Ph.D. Dissertation, University of Zürich Irchel, Zürich.

Specht M, Lebrun R, Zollikofer CPE (2007) Visualizing shape transformation between chimpanzee and human braincases. *The Visual Computer* **23**, 743–751.

Spoor C (1993) The comparative morphology and phylogeny of the human bony labyrinth. Ph.D. Dissertation, Utrecht University, The Netherlands.

Spoor F, Zonneveld F (1995) Morphometry of the primate bony labyrinth: a new method based on high-resolution computed tomography. *J Anat* **186**, 271–286.

Spoor C, Zonneveld F (1998) Comparative review of the human bony labyrinth. *Am J Phys Anthropol* **41**, 211–251.

Spoor F, Wood B, Zonneveld F (1994) Implications of early hominid labyrinthine morphology for evolution of human bipedal locomotion. *Nature* **369**, 645–648.

Spoor C, Bajpai S, Hussain ST, et al. (2002) Vestibular evidence for the evolution of aquatic behaviour in early cetaceans. *Nature* **417**, 163–166.

Spoor C, Hublin J-J, Braun M, et al. (2003) The bony labyrinth of Neanderthals. *J Human Evol* **44**, 141–165.

Spoor F, Garland TJ, Krovitz G, et al. (2007) The primate semicircular canal system and locomotion. *Proc Natl Acad Sci U S A* **104**, 10808–10812.

Steele CR, Zais JG (1985) Effect of coiling in a cochlear model. *J Acoust Soc Am* **77**, 1849–1852.

Tafforeau P, Boistel R, Boller E, et al. (2006) Applications of X-ray synchrotron microtomography for non-destructive 3D studies of paleontological specimens. *Appl Phys Mat Sci Process* **83**, 195–202.

Tavaré S, Marshall CR, Will O, et al. (2002) Using the fossil record to estimate the age of the last common ancestor of extant primates. *Nature* **416**, 726–729.

Waddell PJ, Cao Y, Hasegawa M, et al. (1999) Assessing the Cretaceous superordinal divergence times within birds and placental mammals by using whole mitochondrial protein sequences and an extended statistical framework. *Syst Biol* **48**, 119–137.

Walker A, Ryan TM, Silcox MT, et al. (2008) The semicircular canal system and locomotion: the case of extinct lemuroids and lorisoids. *Evol Anthropol* **17**, 135–145.

West CD (1985) The relationship of the spiral turns of the cochlea and the length of the basilar membrane to the range of audible frequencies in ground dwelling mammals. *J Acoust Soc Am* **77**, 1091–1100.

Wiley DF, Amenta N, Alcantara DA, et al. (2005) Evolutionary morphing. *Proc IEEE Vis*, 431–438.

Yoder AD (1997) Back to the future: a synthesis of Strepsirrhine systematics. *Evol Anthropol* **6**, 11–22.

Yoder AD, Yang Z (2004) Divergence dates for Malagasy lemurs estimated from multiple gene loci: geological and evolutionary context. *Mol Ecol* **13**, 757–773.

Yoder AD, Cartmill M, Ruvolo M, et al. (1996) Ancient single origin for Malagasy primates. *Proc Natl Acad Sci U S A* **93**, 5122–5126.

Yoder AD, Rasoloarison RM, Goodman SM, et al. (2000) Remarkable species diversity in Malagasy mouse lemurs (primates, *Microcebus*). *Proc Natl Acad Sci U S A* **97**, 11325–11330.

Supporting Information

Additional Supporting Information may be found in the online version of this article:

Fig. S1. Medial axis transform of labyrinthine morphology. (A) Initial 3D mesh representation of the bony labyrinth. (B) Raw medial axis produced by the Power Crust algorithm (Amenta et al. 2001). (C) Simplified version of the approximate medial axis. (D) Original 3D mesh, simplified version of the medial axis and corresponding landmark positions. Specimen: *Lepilemur ruficaudatus* AIM-ZU 11054.

Fig. S2. Landmarks used for geometric morphometric analysis of the whole cranium, the face, the neurocranium and the basicranium. Specimen: *Lepilemur ruficaudatus* AIM-ZU 11054.

Fig. S3. Sample mean labyrinthine shape. According to a random-walk model of evolution of characters, the sample mean shape best approximates the LCA state of all strepsirrhine primates. The inner ear of *Lepilemur ruficaudatus* AIM-ZU 11054 was used as a template.

Fig. S4. Left bony labyrinth of *Pseudopotto martini* (A) and *Otolemur crassicaudatus* (B). Labyrinths are represented in superior view, the horizontal plane being the lateral semicircular canal. Scale bar is 1 mm. Arrow: in most Galagidae (example: *Otolemur crassicaudatus*), the lateral semicircular canal is so large that it intersects with the plane formed by the posterior semicircular canal, a condition which is not encountered in species exhibiting relatively small lateral semicircular canals, such as the Lorisidae (example: *Pseudopotto martini*). Specimens: AIM-ZU 6698 (*Pseudopotto martini*) and AIM-ZU 1841 (*Otolemur crassicaudatus*).

As a service to our authors and readers, this journal provides supporting information supplied by the authors. Such materials are peer-reviewed and may be re-organized for online delivery, but are not copy-edited or typeset. Technical support issues arising from supporting information (other than missing files) should be addressed to the authors.